Thermally responsive poly(ethylene oxide)-based polyrotaxanes bearing hydrogen-bonding pillar [5] arene rings

Kenichi Kato
Kyoto University
Katsuto Onishi
Kyoto University
Koki Maeda
Kyoto University
Masafumi Yagyu
Kanazawa University
Shixin Fa
Kyoto University
Takahiro Ichikawa
Tokyo University of Agriculture and Technology
Motohiro Mizuno
Kanazawa University
Takahiro Kakuta
Kanazawa University
Tada-aki Yamagishi
Kanazawa University
Tomoki Ogoshi (ogoshi.tomoki.3s@kyoto-u.ac.jp)
Kyoto University https://orcid.org/0000-0002-4464-0347

Article

Keywords: Poly(ethylene oxide)s, pillar[5]arene rings, polyrotaxanes

Posted Date: October 28th, 2020

DOI: https://doi.org/10.21203/rs.3.rs-85080/v1

Version of Record: A version of this preprint was published at Chemistry – A European Journal on February 5th, 2021. See the published version at https://doi.org/10.1002/chem.202005099.

Abstract

Poly(ethylene oxide)s (PEOs) are useful polymers with good water solubility, biological compatibility, and commercial availability. In this study, PEOs with various end groups were threaded into pillar[5]arene rings in a mixture of water and methanol to afford pseudopolyrotaxanes. Multiple hydrogen bonds between the pillar[5]arene rings and hydrophobic–hydrophilic interactions between the ethylene groups of the PEOs and the hydrophobic pillar[5]arenes are the driving forces to form the pseudopolyrotaxane structure. Corresponding polyrotaxanes were also constructed by capping COOH-terminated pseudopolyrotaxanes with bulky amines, in which multiple hydrogen bonds involving the pillar[5]arene OH groups were critically important to prevent de-threading. The number of threaded ring components could be rationally controlled in these materials, providing a simple and versatile method to tune the mechanical and thermal properties. Specifically, a polyrotaxane with a high-molecular-weight axle became elastic upon heating above the melting point of PEOs and exhibited temperature-dependent shape memory property, because of the topological confinement and cross-linking by hydrogen bonds.

Introduction

Topological supramolecules are materials assembled from geometrically confined or interlocked components instead of rigid covalent bond frameworks. This method of assembly allows for some forms of molecular motion, which endows these supramolecules with unique mechanical and thermal properties.[1−7] Polyrotaxanes, in which many macrocycles are threaded onto a polymer chain and trapped by terminal bulky stoppers, have recently attracted considerable interest for their simple structures and properties different from conventional polymers.[8−13]

Poly(ethylene oxide)s (PEOs) are a class of polymers, which exhibit crystalline and thermoplastic behavior, as well as high solubility in both water and organic solvents. PEOs have a broad scope of applications in materials science and biochemistry because of their excellent biological compatibility and commercial availability in a wide range of molecular weights.[14] Hence, PEO-based supramolecules are of critical importance as an easy and versatile platform for biocompatible materials with tunable properties, which are difficult to be realized using covalently constructed copolymers. The formation of pseudopolyrotaxane and polyrotaxane with PEO axles was accomplished by Harada and co-workers in the 1990s, using α-cyclodextrin (**α-CD**)[15−17] as the ring components (**α-CD•PEO-OH** and **α-CD•PEO-NHAr** in Fig. 1).[8−11,18,19] In these examples, the pseudopolyrotaxanes were collected as precipitates by simply mixing aqueous solution of **α-CD** and that of PEOs. Intermolecular hydrogen bonds between the **α-CDs** and hydrophobic–hydrophilic interactions between the hydrophobic ethylene groups of the PEOs and **α-CD** cavity are the driving forces to form the pseudopolyrotaxane structure. However, these interactions between the PEOs and cyclic host molecules are generally weak compared with the high affinity of PEOs for various solvents, leading to difficulties in capturing PEO chains within molecule-based nanometer spaces.[20−23] Additionally, the free space of these cyclic hosts often needs to be activated in advance, hampering the formation of rotaxanes via a solution process. Considering the great success of

supramolecular polymer materials composed of PEOs and cyclodextrins,[24–30] alternative cyclic hosts for PEO axles are highly desirable for the further development of PEO-based hydrogels and other functional materials.

Pillar[n]arenes are macrocyclic molecules in which *para*-hydroquinone π-panels are linked together via methylene bridges.[31–39] Owing to the electron-rich cavity, these compounds exhibit excellent host–guest properties to form complexes, not only with cationic compounds by charge-transfer interactions, but also with neutral molecules, including non-functionalized alkanes, via multiple CH–π interactions. Pillar[n]arenes have also been used to construct pseudopolyrotaxanes and polyrotaxanes with polymeric viologen, polyaniline, poly(tetrahydrofuran), and polyethylene as the axle components.[40–45] Although an activated crystal of per-ethylated pillar[5]arene **P5OEt** (Fig. 1) took up some PEO chains in its one-dimensional channels when it was immersed in melted PEO, no host–guest complexation between PEOs and **P5OEt** was detected by ^{1}H NMR studies in $CDCl_3$.[22] The use of aqueous media is a promising method, but common alkylated pillar[n]arenes are insoluble in water, unlike **α-CD**. In this study, PEOs were threaded into the non-alkylated pillar[5]arene **P5OH** in a mixture of water and methanol to yield pseudopolyrotaxanes. This method can be applied to PEOs with various molecular weights and terminal functionalities, which allows for the construction of polyrotaxanes by capping the PEO end groups with bulky amines. Because of the hydrogen-bond networks involving the phenolic pillar[5]arene OHs, a polyrotaxane with a high-molecular-weight PEO axle exhibited elasticity at temperatures above the melting point of the PEOs.

Results

Formation of pseudopolyrotaxanes. First, we envisioned using non-alkylated pillar[5]arene **P5OH**[46] as the ring components of PEO-based pseudopolyrotaxanes (Fig. 2a). Because of the 10 phenolic OH groups, **P5OH** is able to form effective hydrogen bonds and is partially soluble in aqueous media, unlike alkylated pillar[n]arene derivatives. In this study, **P5OH** was dissolved in a mixture of water and methanol [1/1 (v/v)], to which was added a solution of OH-terminated PEO (molecular weight: 2000) **PEO2k-OH** in the same solvent system. Threading of **PEO2k-OH** into **P5OH** yielded the pseudopolyrotaxane **P5OH•PEO2k-OH** as a precipitate owing to its decreased solubility in the mixed solvent (Supplementary Movie 1). The obtained solids were washed with water to remove free **P5OH** and **PEO2k-OH** and slowly dried by heating at 60 °C in air.

Pseudopolyrotaxane **P5OH•PEO2k-OH** was dissolved in acetone-d_6 and characterized by ^{1}H NMR spectroscopy (Supplementary Fig. 2). Sharp peaks from dissociated **P5OH** and **PEO2k-OH** appeared at 7.96, 6.67, and 3.59 ppm as a consequence of de-threading.[46] On the basis of the integral values, the molar ratio of ethylene oxide (EO) units to **P5OH** was estimated to be 8. A solid sample of **P5OH•PEO2k-OH** was also investigated by solid-state 2D ^{1}H/^{13}C hetero-correlated NMR spectroscopy with magic angle spinning (Fig. 3a). Cross-peaks were detected between the ^{1}H signals due to **P5OH** and the ^{13}C signal due to **PEO2k-OH** at 69.7 ppm. These intermolecular correlations clearly indicated the proximity of the two

components. Furthermore, the observed ^{13}C peak was shifted to higher field than the peaks of the crystalline and non-crystalline PEOs (71.2 and 72.0 ppm, respectively).[47,48] This peak shift could be rationalized in terms of aromatic shielding, thereby indicating that complexation between the PEO chains and pillar[5]arene rings had occurred.[22]

Powder X-ray diffraction (PXRD) analysis was performed for **P5OH•PEO2k-OH** and its components, **P5OH** and **PEO2k-OH**, to investigate the solid-state structures (Fig. 3b). While the solid sample of each component showed several sharp peaks in the PXRD pattern, the pattern for the pseudopolyrotaxane **P5OH•PEO2k-OH** was composed of unclear signals. These results indicated the absence of uncomplexed **P5OH** and **PEO2k-OH** and the formation of a non-crystalline complex. The absence of free **P5OH** in the pseudopolyrotaxane sample was also confirmed by the lack of CO_2 gas adsorption behavior (Supplementary Fig. 18).

Threading into **P5OH** changed the assembled structures of the PEOs to cause a large perturbation in the thermal properties. In differential scanning calorimetry (DSC) studies, **P5OH•PEO2k-OH** showed no explicit signals from − 70 °C to 100 °C, while **PEO2k-OH** had endothermic and exothermic peaks at 53 and 25 °C, because of the melting and crystallization of the pristine PEO (Supplementary Fig. 20). The disappearance of the melting behavior of PEO was highly dependent on the number of threaded ring units. The molar ratio of EO units to **P5OH** could be rationally controlled by changing the amount of added PEO solution in the preparation (Supplementary Table 2), providing pseudopolyrotaxanes with EO-to-**P5OH** ratios of 8–23. As the number of EO units increased from 8 to 15, endothermic peaks gradually became evident and shifted to lower temperatures (Supplementary Fig. 21). Thermogravimetric analysis (TGA) in air was also performed for **P5OH•PEO2k-OH** along with its uncomplexed components (Supplementary Fig. 23). The 10% weight loss temperatures were 164, 229, and 302 °C for **P5OH**, **PEO2k-OH**, and **P5OH•PEO2k-OH**, respectively, clearly indicating an improvement in the thermal stability upon complexation.

To obtain further insight into the pseudopolyrotaxane formation, we prepared **P5OH•PEO2k-OH** in the presence of adiponitrile as a competitive guest. The yield of pseudopolyrotaxanes decreased from 32–3.2% and the molar ratio of EO units to **P5OH** was increased from 8 to 27 as a result of ineffective threading. Pseudopolyrotaxane formation was also hampered when the pH of the solvent system was increased to 12 using NaOH (yield: 8.8%; EO-to-**P5OH** ratio: 193). Such basic conditions cause deprotonation of **P5OH** to generate anionic species, which experience charge repulsion with one another. Additionally, we tested the preparation of the pseudopolyrotaxane using pure methanol instead of the mixed solvent but could not obtain any precipitate. Hence, hydrophobic–hydrophilic interactions between the hydrophobic ethylene groups of the PEOs and pillar[5]arenes are thought to be a major driving force to form the pseudopolyrotaxane structure, in addition to the multiple hydrogen bonds between the pillar[5]arene rings. Alteration of the terminal groups of the PEOs did not appreciably affect the threading into the **P5OH** rings, and amine-, methoxy-, and tosylate-terminated pseudopolyrotaxanes were able to be constructed (Fig. 2a). Further, **PEO2k-OH** could be replaced with PEOs with larger molecular weights up to 500,000 (Supplementary Table 3). As the PEO molecular weight increased, the yield of

pseudopolyrotaxane and EO-to-**P5OH** ratio tended to increase probably because of decreased solubility in the mixed solvent.

Synthesis of polyrotaxanes. Encouraged by the versatility in PEO axles, we next attempted the synthesis of polyrotaxanes composed of **P5OH** and PEOs (Fig. 2b). Following the procedure described above, pseudopolyrotaxane **P5OH•PEO20k-COOH** with an EO-to-**P5OH** ratio of 4.2 was prepared in 19% yield, and then the terminal carboxylic acid groups were capped by condensation with 1-adamantanamine in acetone, with the assistance of BOP reagent and EDIPA.[49] Before the completion of the amide formation, some ring units were de-threaded and the resulting free **P5OH** and **PEO20k-COOH** were dissolved in acetone. In contrast, the capped polyrotaxane **P5OH•PEO20k-CONHAd** was not very soluble in acetone, enabling purification by simple washing with acetone. Intermolecular hydrogen bonds involving **P5OH** would prevent the solvation in acetone. The polyrotaxane was soluble in a limited number of solvents, including DMF, DMSO, and basic water. Similar results have been also reported for polyrotaxanes constructed from **α-CD** and PEO.[19]

The ^{1}H NMR spectrum of **P5OH•PEO20k-CONHAd** was recorded in DMSO-d_6 (Fig. 4a). The peaks due to the **P5OH** units at 7.58–6.60 ppm were complicatedly split owing to the presence of several conformers, which indicated that threading of the PEO resulted in frozen rotation of the **P5OH** π-panels. The molar ratio of EO units to **P5OH** was determined to be 9 from the integral values. In gel permeation chromatography (GPC) analysis, broad **P5OH**-derived UV absorption peaks were detected in a higher molecular weight region than the peak of uncomplexed **P5OH** (Fig. 4b). CO_2 gas adsorption behavior derived from free **P5OH** was also disappeared in **P5OH•PEO20k-CONHAd** (Supplementary Fig. 19). These results demonstrated the existence of complexed **P5OH** and absence of cavity-free **P5OH**, thereby confirming the formation of a polyrotaxane.

Polyrotaxanes were also synthesized using THF, DMF, and acetonitrile as solvents for the capping reaction, which resulted in decreased yields and decreased numbers of threaded **P5OH** units (Supplementary Table 4). Effects of EO-to-**P5OH** ratios on the thermal properties of polyrotaxanes were evaluated by TGA (Supplementary Fig. 24). Additionally, synthesis of a polyrotaxane with **P5OEt** rings was attempted using the corresponding pseudopolyrotaxane prepared by the immersion method,[22] which was unsuccessful because of facile de-threading (Supplementary Fig. 15). These results exemplified the critical importance of hydrogen bonds for stable complexation in organic solvents and indicated that cleavage was mediated by polar solvents, which promoted de-threading and solubilizing processes.

Thermal and mechanical properties of a high-molecular-weight polyrotaxane. A polyrotaxane with a high-molecular-weight PEO axle, **P5OH•PEO500k-CONHAd** (EO-to-**P5OH** ratio: 28), was prepared using acetone as the solvent, as well as the **α-CD** counterpart **α-CD•PEO500k-CONHAd**. From the TGA results, the 10% weight loss temperatures were determined to be 275 and 355 °C for the **α-CD**- and **P5OH**-based polyrotaxanes, respectively (Supplementary Fig. 25). The improved thermal stability of **P5OH•PEO500k-CONHAd** was attributed to the rigid aromatic structure of **P5OH** as compared with cyclodextrins, which are composed of sugar units linked via fragile acetal bonds.

DSC measurements were also performed for these polyrotaxanes and the parent **PEO500k-COOH** (Fig. 5a and Supplementary Fig. 22). While **α-CD•PEO500k-CONHAd** did not show any peaks in the region of 0–160 °C, **P5OH•PEO500k-CONHAd** showed two sets of endothermic/exothermic peaks at 50.7/27.2 and 60.3/42.0 °C. The peaks at higher temperatures were attributed to the melting behavior of naked parts of PEO chains and the remaining broad peaks were ascribed to EO units near **P5OH** rings. Importantly, **P5OH•PEO500k-CONHAd** did not melt upon heating over 60.3 °C, but exhibited thermoplastic behavior while retaining a solid state, which could be rationalized by the presence of multiple hydrogen bonds. Because of this thermo-responsive mechanical property, heating to 125 °C allowed the shape of **P5OH•PEO500k-CONHAd** to be altered, which was retained at room temperature and then was returned to the original form when it was heated again to 125 °C (Fig. 5b and Supplementary Movie 2). This shape memory property was also investigated in terms of variable-temperature PXRD patterns (Fig. 5c and Supplementary Fig. 17). At 30 °C, **P5OH•PEO500k-CONHAd** showed two peaks at $2\theta = 19.2$ and 23.4°, which disappeared between 60–80 °C in the heating scan and were retrieved between 60–40 °C in the following cooling scan. This behavior was almost the same as that of the parent **PEO500k-COOH**, which suggested that the temperature-dependent mechanical response can be attributed to the local melting process of the PEO chains.

Discussion

We have developed versatile methods for the preparation of pseudopolyrotaxanes assembled from PEOs and **P5OH**, by employing a mixed solvent system of water and methanol. The COOH-terminated pseudopolyrotaxanes could be converted into the corresponding polyrotaxanes. Extensive control experiments confirmed the importance of multiple hydrogen bonds between the pillar[5]arenes and hydrophobic–hydrophilic interactions between the hydrophobic ethylene units of the PEOs and pillar[5]arene as the driving forces to cause threading and prevent de-threading, which is in accordance with the results for **α-CD**-based pseudopolyrotaxanes and polyrotaxanes. Such insights were used to control the number of threaded ring units of the pseudopolyrotaxanes and polyrotaxanes, successfully altering the assembled structures and thermal properties. Therefore, **P5OH**-based pseudopolyrotaxanes and polyrotaxanes have the potential to be used in simple and versatile materials because a wide range of PEOs are commercially available and are used as water-soluble and biocompatible materials, including those combined with **α-CD**s.

In the present study, a high-molecular-weight polyrotaxane **P5OH•PEO500k-CONHAd** was also synthesized. Compared with the **α-CD** counterpart, **P5OH•PEO500k-CONHAd** exhibited improved thermal robustness owing to the rigid aromatic framework of **P5OH** instead of the sugar moieties with fragile acetal bonds in **α-CD**. Because of the multiple hydrogen bonds, **P5OH•PEO500k-CONHAd** displayed thermally induced elasticity and shape memory without cross-linking or other late-stage modifications. These properties are in contrast to those of **α-CD**-based polyrotaxanes, with which topological hydrogels were produced by cross-linking **α-CD** components with additional chemical bonds.[50–52] These results indicate the utility of **P5OH**-based polyrotaxanes and we believe that novel supramolecular materials[53–

[57] can be produced based on the hydrogen-bonding character and further functionalization of the ring units.

Methods

Materials. All solvents and reagents were of commercial reagent grade and were used without further purification except where noted. Super dehydrated acetone and acetonitrile were purchased from FUJIFILM Wako Pure Chemical Co., Osaka, Japan. Dry THF and DMF were purchased from KANTO CHEMICAL CO.,INC. Supplementary Table 1 shows the product information for poly(ethylene oxide)s (PEOs) used in this study. Pillar[5]arene bearing 10 hydroxy groups (**P5OH**) was synthesized according to a previous paper.[46] COOH-terminated PEOs (**PEO20k-COOH** and **PEO500k-COOH**) were prepared in 91% and 76% yields, respectively, following the reported methods[49] with minor modification (see Supplementary information). Sonication was conducted with an ultrasonic cleaner BRANSON M5800-J. Centrifugation was performed on a centrifuge KOKUSAN H-36α.

Preparation of the pseudopolyrotaxane of P5OH and PEO (P5OH•PEO2k-OH). **P5OH** (0.075 g, 0.10 mmol) was dissolved in a mixed solvent of methanol and water (10 mL, 1/1 (v/v), 10 mmol/L) in a 50-mL centrifuge vial. Polyethylene Glycol 2,000 (**PEO2k-OH**, 0.500 g, 0.25 mmol) was also dissolved in the same mixed solvent (6.0 mL, 42 mmol/L) in another vial. The **PEO2k-OH** solution (0.60 mL) was added to the **P5OH** solution (10 mL) and the resulting mixture was vigorously sonicated for 1 h. The mixture was allowed to stand overnight and then centrifuged. The resulting supernatant was removed to give the crude pseudopolyrotaxane as a precipitate. The precipitate was washed with water and dried *in vacuo*, affording pseudopolyrotaxane (**P5OH•PEO2k-OH**, 0.040 g, 32%, powder). Pseudopolyrotaxane **P5OH•PEO2k-OH** was dissolved in acetone-d_6 to provide a set of ^{1}H NMR signals from the dissociated **P5OH** and **PEO2k-OH**. From the ratio of the integral values, the molar ratio of ethylene oxide (EO) units to **P5OH** was estimated to be 8.

Synthesis of the polyrotaxanes of P5OH and PEO (P5OH•PEO20k-CONHAd). 1-Adamantanamine (16 mg, 0.11 mmol), (benzotriazol-1-yloxy)tris(dimethylamino)-phosphonium hexafluorophosphate (BOP reagent, 48 mg, 0.11 mmol), and *N*-ethyldiisopropylamine (EDIPA, 0.019 mL, 0.12 mmol) were dissolved in super dehydrated acetone (10 mL). The solution was cooled to 0 °C with an ice bath, to which **P5OH•PEO20k-COOH** (152 mg) was added. The reaction mixture was allowed to warm up to room temperature and stirred overnight at that temperature. After the solvent was removed under reduced pressure, the residue was washed with acetone to yield **P5OH•PEO20k-CONHAd** (66 mg, 43%) as a brown solid. On the basis of the same procedure, **P5OH•PEO500k-CONHAd** (100 mg, EO-to-**P5OH** ratio: 28) was obtained in 33% yield from **P5OH•PEO500k-COOH** (300 mg).

NMR spectroscopy. ^{1}H NMR spectra were recorded on a JEOL ECA-400 spectrometer. Chemical shifts were reported as the delta scale in ppm relative to tetramethylsilane (TMS, δ = 0.00 ppm) as the internal standard. Solid-state ^{13}C NMR spectrum was measured using a JEOL ECA-300 spectrometer operating at 74.175 MHz. High-resolution solid-state NMR spectrum was obtained using magic-angle spinning (MAS)

and high-power ^{1}H dipole decoupling (DD). Cross-polarization (CP) was used for signal enhancement. The sample was packed into a 4 mm diameter zirconia rotor. The MAS rate was set to 5 kHz. ^{13}C chemical shifts were expressed as values relative to tetramethylsilane (TMS) using the 29.50 ppm line of adamantane as an external reference. In the 2D ^{1}H–^{13}C heterocorrelated NMR measurement, the ^{1}H signals were detected using Phase Modulated Lee–Goldburg (PMLG) homonuclear decoupling.[58]

Gel permeation chromatography (GPC) analysis. When THF was used as the eluent, gel permeation chromatography (GPC) analysis was performed at 25 °C on a Shodex GPC LF804 system at a flow rate of 1 mL·min^{-1}. In the case of DMF (10 mM LiBr) as the eluent, GPC analysis was performed at 40 °C on a TOSHO TSKgel α-3000 at a flow rate of 1 mL·min^{-1}.

Powder X-ray diffraction (PXRD) analysis. Powder X-ray diffraction (PXRD) measurements were performed on a Rigaku Smart Lab high-resolution diffractometer.

CO_2 adsorption measurements. The amount of CO_2 adsorption was measured using a BELSORP-max-12-N-VP-K (BEL Japan Inc., Osaka, Japan).

Differential scanning calorimetry (DSC). DSC curves were recorded on a DSC7020 (Hitachi High-Tech Science Co., Tokyo, Japan).

Thermogravimetric analysis (TGA). TGA results were obtained by a STA7200 (Hitachi High-Tech Science Co., Tokyo, Japan).

References

1. Fang, L. et al. Mechanically bonded macromolecules. *Chem. Soc. Rev.* **39**, 17–29 (2010).
2. van Dongen, S. F. M., Cantekin, S., Elemans, J. A. A. W., Rowan, A. E. & Nolte, R. J. M. Functional interlocked systems. *Chem. Soc. Rev.* **43**, 99–122 (2014).
3. He, Z., Jiang, W. & Schalley, C. A. Integrative self-sorting: a versatile strategy for the construction of complex supramolecular architecture. *Chem. Soc. Rev.* **44**, 779–789 (2015).
4. Qu, D.-H., Wang, Q.-C., Zhang, Q.-W., Ma, X. & Tian, H. Photoresponsive Host – Guest Functional Systems. *Chem. Rev.* **115**, 7543–7588 (2015).
5. Erbas-Cakmak, S., Leigh, D. A., McTernan, C. T. & Nussbaumer, A. L. Artificial Molecular Machines. *Chem. Rev.* **115**, 10081–10206 (2015).
6. Takata, T. Switchable Polymer Materials Controlled by Rotaxane Macromolecular Switches. *ACS Cent. Sci.* **6**, 129–143 (2020).
7. Baroncini, M., Silvi, S. & Credi, A. Photo- and Redox-Driven Artificial Molecular Motors. *Chem. Rev.* **120**, 200–268 (2020).
8. Huang, F. & Gibson, H. W. Polypseudorotaxanes and polyrotaxanes. *Prog. Polym. Sci.* **30**, 982–1018 (2005).

9. Wenz, G., Han, B.-H. & Müller, A. Cyclodextrin Rotaxanes and Polyrotaxanes. *Chem. Rev.* **106**, 782–817 (2006).
10. Harada, A., Hashidzume, A., Yamaguchi, H. & Takashima, Y. Polymeric Rotaxanes. *Chem. Rev.* **109**, 5974–6023 (2009).
11. Arunachalam, M. & Gibson, H. W. Recent developments in polypseudorotaxanes and polyrotaxanes. *Prog. Polym. Sci.* **39**, 1043–1073 (2014).
12. Takata, T. Polyrotaxane and Polyrotaxane Network: Supramolecular Architectures Based on the Concept of Dynamic Covalent Bond Chemistry. *Polym. J.* **38**, 1–20 (2006).
13. Zhao, W. et al. Linear Supramolecular Polymers Driven by Anion–Anion Dimerization of Difunctional Phosphonate Monomers Inside Cyanostar Macrocycles. *J. Am. Chem. Soc.* **141**, 4980–4989 (2019).
14. Bailey, F. E. & Koleske, J. V. (eds) *Poly(Ethylene Oxide)* (Academic Press, New York, 1976).
15. Wenz, G. Cyclodextrins as Building Blocks for Supramolecular Structures and Functional Units. *Angew. Chem. Int. Ed. Engl.* **33**, 803–822 (1994).
16. Martin Del Valle, E. M. Cyclodextrins and their uses: a review. *Process Biochem.* **39**, 1033–1046 (2004).
17. Crini, G. Review: A History of Cyclodextrins. *Chem. Rev.* **114**, 10940 – 10975 (2014).
18. Harada, A. & Kamachi, M. Complex Formation between Poly(ethylene glycol) and α-Cyclodextrin. *Macromolecules* **23**, 2821–2823 (1990).
19. Harada, J., Li, J. & Kamachi, M. The molecular necklace: a rotaxane containing many threaded α-cyclodextrins. *Nature* **356**, 325–327 (1992).
20. Uemura, T. et al. Unveiling thermal transitions of polymers in subnanometre pores. *Nat. Commun.* **1**, 83 (2010).
21. Yamashina, M., Kusaba, S., Akita, M., Kikuchi, T. & Yoshizawa, M. Cramming versus threading of long amphiphilic oligomers into a polyaromatic capsule. *Nat. Commun.* **9**, 4227 (2018).
22. Ogoshi, T. et al. Molecular weight fractionation by confinement of polymer in one-dimensional pillar[5]arene channels. *Nat. Commun.* **10**, 479 (2019).
23. Ke, H. et al. Shear-induced assembly of a transient yet highly stretchable hydrogel based on pseudopolyrotaxanes. *Nat. Chem.* **11**, 470–477 (2019).
24. Harada, A. Cyclodextrin-Based Molecular Machines. *Acc. Chem. Res.* **34**, 456–464 (2001).
25. Harada, A., Takashima, Y. & Yamaguchi, H. Cyclodextrin-based supramolecular polymers. *Chem. Soc. Rev.* **38**, 875–882 (2009).
26. Tan, S., Ladewig, K., Fu, Q., Blencowe, A. & Qiao, G. G. Cyclodextrin-Based Supramolecular Assemblies and Hydrogels: Recent Advances and Future Perspectives. *Macromol. Rapid Commun.* **35**, 1166–1184 (2014).
27. Schmidt, B. V. K. J. & Barner-Kowollik, C. B. Dynamic Macromolecular Material Design—The Versatility of Cyclodextrin-Based Host–Guest Chemistry. *Angew. Chem. Int. Ed.* **56**, 8350–8369 (2017).

28. Yan, X., Huang, P. & Nie, Z. Cyclodextrin-based polymer materials: From controlled synthesis to applications. *Prog. Polym. Sci.* **93**, 1–35 (2019).
29. Hashidzume, A., Yamaguchi, H. & Harada, A. Cyclodextrin-Based Rotaxanes: from Rotaxanes to Polyrotaxanes and Further to Functional Materials. *Eur. J. Org. Chem.* 3344–3357 (2019).
30. Domiński, A., Konieczny, T. & Kurcok, P. α-Cyclodextrin-Based Polypseudorotaxane Hydrogels. *Materials* **13**, 133 (2020).
31. Ogoshi, T. (ed) *Pillararene* (The Royal Society of Chemistry, Cambridge, U.K., 2016).
32. Cragg, P. J. & Sharma, K. Pillar[5]arenes: fascinating cyclophanes with a bright future. *Chem. Soc. Rev.* **41**, 597–607 (2012).
33. Xue, M., Yang, Y., Chi, X., Zhang, Z. & Huang, F. Pillararenes, A New Class of Macrocycles for Supramolecular Chemistry. *Acc. Chem. Res.* **45**, 1294–1308 (2012).
34. Stutt, N. L., Huacheng, H., Schneebeli, S. T. & Stoddart, J. F. Functionalizing Pillar[*n*]arenes. *Acc. Chem. Rev.* **47**, 2631–2642 (2014).
35. Ogoshi, T. & Yamagishi, T.-a. Pillar[5]- and pillar[6]arene-based supramolecular assemblies built by using their cavity-size-dependent host–guest interactions. *Chem. Commun.* **50**, 4776–4787 (2014).
36. Li, C. Pillararene-based supramolecular polymers: from molecular recognition to polymeric aggregates. *Chem. Commun.* **50**, 12420–12433 (2014).
37. Yang, K., Pei, Y., Wen, J. & Pei, Z. Recent advances in pillar[*n*]arenes: synthesis and applications based on host–guest interactions. *Chem. Commun.* **52**, 9316–9326 (2016).
38. Ogoshi, T., Yamagishi, T.-a. & Nakamoto, Y. Pillar-Shaped Macrocyclic Hosts Pillar[n]arenes: New Key Players for Supramolecular Chemistry. *Chem. Rev.* **116**, 7937–8002 (2016).
39. Ogoshi, T., Kakuta, T. & Yamagishi, T.-a. Applications of Pillar[n]arene-Based Supramolecular Assemblies. *Angew. Chem. Int. Ed.* **58**, 2197–2206 (2019).
40. Ogoshi, T., Nishida, Y., Yamagishi, T.-a. & Nakamoto, Y. Polypseudorotaxane Constructed from Pillar[5]arene and Viologen Polymer. *Macromolecules* **43**, 3145–3147 (2010).
41. Ogoshi, T., Nishida, Y., Yamagishi, T.-a. & Nakamoto, Y. High Yield Synthesis of Polyrotaxane Constructed from Pillar[5]arene and Viologen Polymer and Stabilization of Its Radical Cation. *Macromolecules* **43**, 7068–7072 (2010).
42. Ogoshi, T. et al. Reduction of Emeraldine Base Form of Polyaniline by Pillar[5]arene Based on Formation of Poly(pseudorotaxane) Structure. *Macromolecules* **44**, 7639–7644 (2011).
43. Ogoshi, T., Aoki, T., Ueda, S., Tamura, Y. & Yamagishi, T.-a. Pillar[5]arene-based nonionic polyrotaxanes and a topological gel prepared from cyclic host liquids. *Chem. Commun.* **50**, 6607–6609 (2014).
44. Ogoshi, T. et al. Extension of polyethylene chains by formation of polypseudorotaxane structures with perpentylated pillar[5]arenes. *Polym. J.* **46**, 77–81 (2014).
45. Chen, J. et al. Dual-responsive polypseudorotaxanes based on block-selected inclusion between polyethylene-block-poly(ethylene glycol) diblock copolymers and 1,4-diethoxypillar[5]arene. *Soft*

Matter **11**, 7835–7840 (2015).

46. Ogoshi, T., Kanai, S., Fujinami, S., Yamagishi & T.-a.; Nakamoto, Y. *para*-Bridged Symmetrical Pillar[5]arenes: Their Lewis Acid Catalyzed Synthesis and Host–Guest Property. *J. Am. Chem. Soc.* **130**, 5022–5023 (2008).
47. Yamamoto, K., Murata, A. & Shimada, S. Structure and molecular motion of poly(ethylene oxide) chains tethered on silica by solid state ^{13}C NMR method. *Polym. J.* **33**, 584–589 (2001).
48. Schantz, S. Structure and mobility in poly(ethylene oxide)/poly(methyl methacrylate) blends investigated by ^{13}C solid-state NMR. *Macromolecules* **30**, 1419–1425 (1997).
49. Araki, J., Zhao, C. & Ito, K. Efficient Production of Polyrotaxanes from α-Cyclodextrin and Poly(ethylene glycol). *Macromolecules* **38**, 7524–7527 (2005).
50. Okumura, Y. & Ito, K. The Polyrotaxane Gel: A Topological Gel by Figure-of-Eight Cross-links. *Adv. Mater.* **13**, 485–487 (2001).
51. Karino, T., Okumura, Y., Ito, K. & Shibayama, M. SANS Studies on Spatial Inhomogeneities of Slide-Ring Gels. *Macromolecules* **37**, 6177–6182 (2004).
52. Lin, Q., Hou, X. & Ke, C. Ring Shuttling Controls Macroscopic Motion in a Three-Dimensional Printed Polyrotaxane Monolith. *Angew. Chem. Int. Ed.* **56**, 4452–4457 (2017).
53. Ni, M. et al. Dramatically Promoted Swelling of a Hydrogel by Pillar[6]arene–Ferrocene Complexation with Multistimuli Responsiveness. *J. Am. Chem. Soc.* **138**, 6643–6649 (2016).
54. Wang, S. et al. Warm/cool-tone switchable thermochromic material for smart windows by orthogonally integrating properties of pillar[6]arene and ferrocene. *Nat. Commun.* **9**, 1737 (2018).
55. Li, Z.-Y. et al. Cross-Linked Supramolecular Polymer Gels Constructed from Discrete Multi-pillar[5]arene Metallacycles and Their Multiple Stimuli-Responsive Behavior. *J. Am. Chem. Soc.* **136**, 8577–8589 (2014).
56. Xia, W. et al. Responsive Gel-like Supramolecular Network Based on Pillar[6]arene – Ferrocenium Recognition Motifs in Polymeric Matrix. *Macromolecules* **48**, 4403–4409 (2015).
57. Kardelis, V. et al. Supramolecular Organogels Prepared from Pillar[5]arene-Functionalized Conjugated Polymers. *Macromolecules* **50**, 9144–9150 (2017).
58. Vinogradov, E., Madhu, P. K. & Vega, S. High-resolution proton solid-state NMR spectroscopy by phase-modulated Lee–Goldburg experiment. *Chem. Phys. Lett.* **314**, 443–450 (1999).

Declarations

Acknowledgements

This work was supported by the Grant-in-Aid for Scientific Research on Innovative Areas: p-System Figuration (JP15H00990 and JP17H05148, T.O.), Soft Crystal (JP18H04510 and JP20H04670, T.O.), and Kiban A (19H00909, T.O.) from MEXT Japan, JST CREST (JPMJCR18R3, T.O.), and the World Premier

International Research Center Initiative (WPI), MEXT, Japan. We thank Prof. Kazuo Tanaka and Dr. Shunichiro Ito (Kyoto University) for GPC measurements.

Author contributions

T.O. conceived the project and designed the experiments. K.K., K.O., K.M., M.Y., S.F., T.K., and T.Y. synthesized and characterized the poly(pseudo)rotaxanes with PEO; T.I. measured the variable-temperature powder X-ray diffraction patterns; and M.M. performed the solid-state NMR measurements. All authors analysed and discussed the results, and co-wrote the paper.

Additional information

Supplementary Information accompanies this paper

Competing interests: The authors declare no competing interests.

Figures

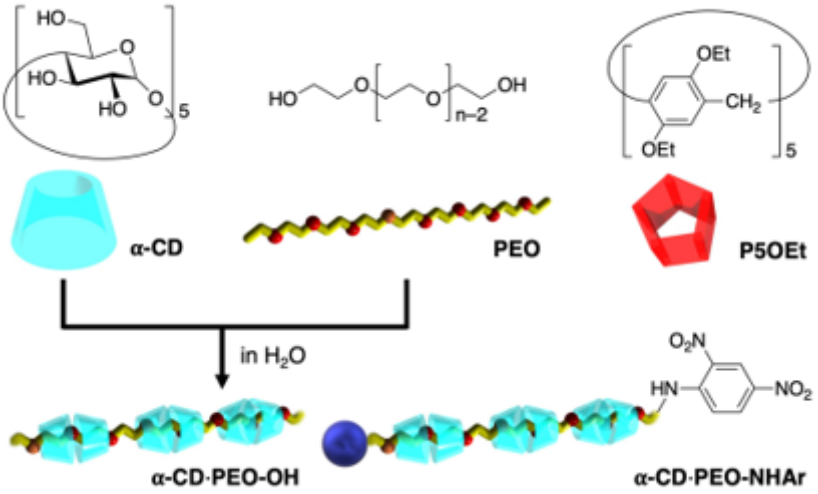

Figure 1

Chemical structures of α-CD, PEO, and P5OEt. PEO-based pseudopolyrotaxane and polyrotaxane

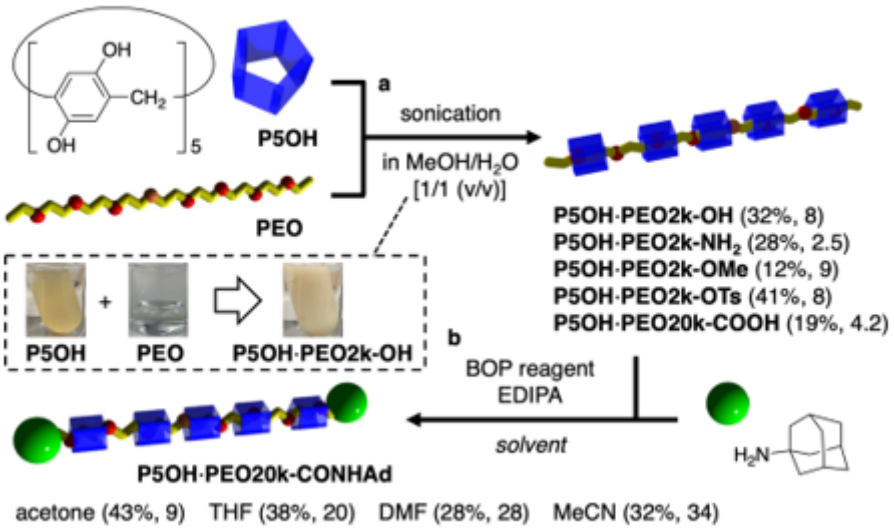

Figure 2

a Preparation of pseudopolyrotaxanes assembled from pillar[5]arene and poly(ethylene oxide)s and b conversion to polyrotaxanes. Yields and EO-to-P5OH ratios are given in brackets. BOP reagent = (benzotriazol-1-yloxy)tris(dimethylamino)phosphonium hexafluorophosphate, EDIPA = N-ethyldiisopropylamine

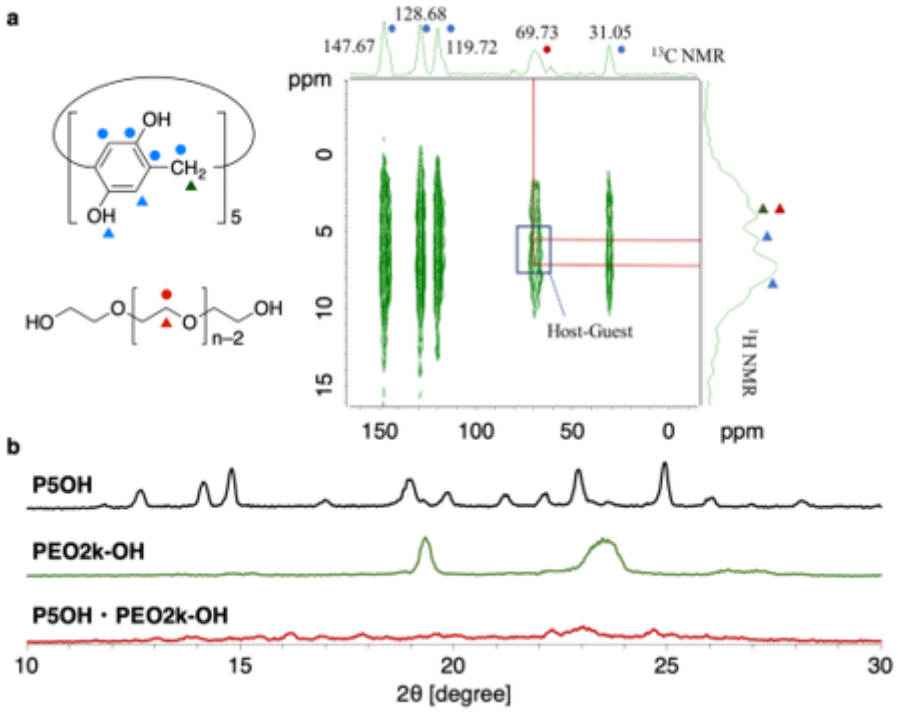

Figure 3

a Solid-state 2D 1H/13C hetero-correlated NMR spectrum of P5OH•PEO2k-OH and b PXRD patterns of P5OH (top), PEO2k-OH (middle), and P5OH•PEO2k-OH (bottom)

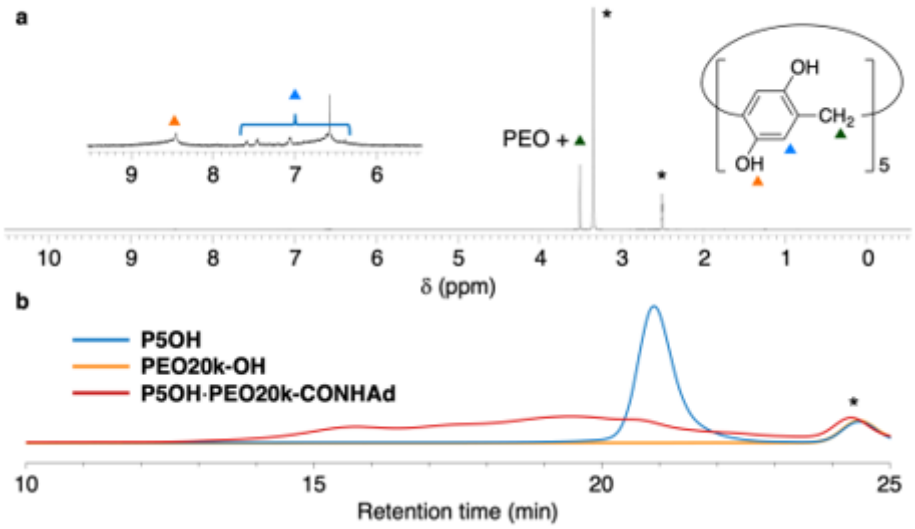

Figure 4

a 1H NMR spectrum of P5OH•PEO20k-CONHAd in DMSO-d6 at 25 °C. Peaks marked with * are due to residual solvent. The inset shows the aromatic region, in which split signals were assigned to various conformers of P5OH fixed by complexation with PEO. b GPC charts of P5OH (blue), PEO20k-OH (orange), and P5OH•PEO20k-CONHAd (red) of absorption of 270-nm UV light. Peaks marked with * are due to DMF

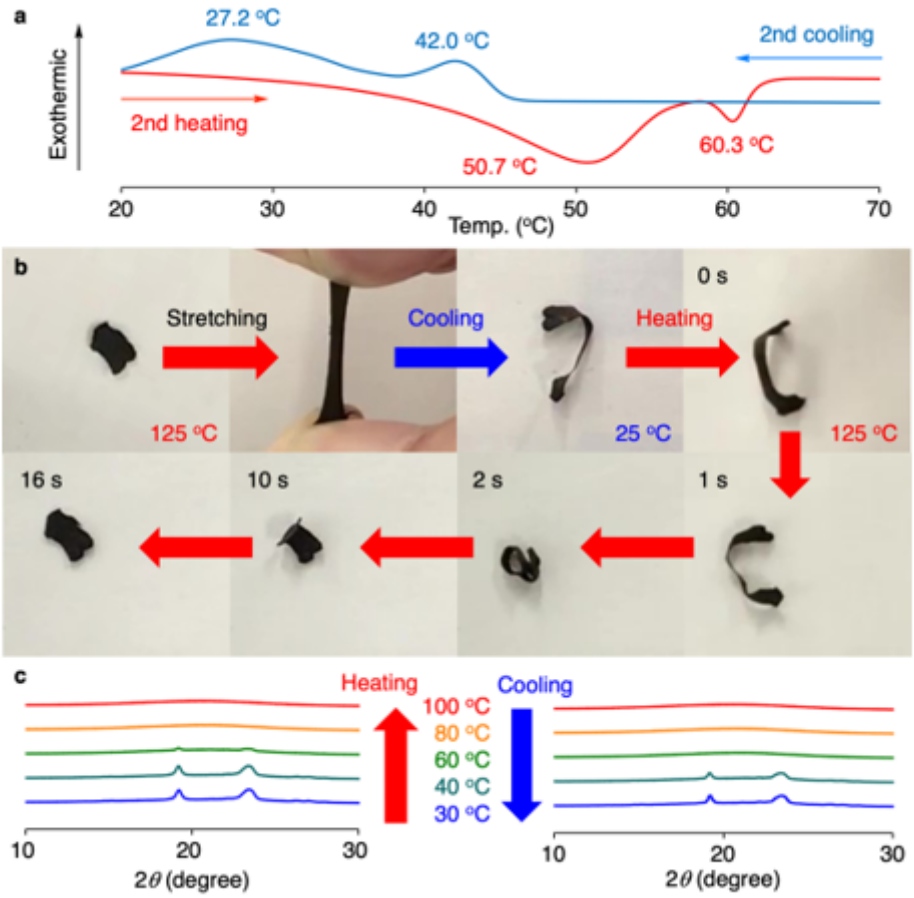

Figure 5

Thermal and mechanical properties of P5OH•PEO500k-CONHAd. a DSC chart. b Change in mechanical response. By stretching upon heating (125 °C) then cooling (25 °C), the shape of an extended film was fixed, then went back to the initial shape upon heating again. c Variable-temperature PXRD patterns

Supplementary Files

This is a list of supplementary files associated with this preprint. Click to download.

- movieS1.mov
- movieS2.mov
- SI5OHPEGncomms0928kk.docx